ACCSCIENCE PUBLISHING

Eurasian Journal of Medicine and Oncology

ORIGINAL RESEARCH ARTICLE

Ai Da Lotion improves eczema lesions via modulation of the JAK1/STAT3 pathway and regulation of apoptosis and oxidative stress

Yuan Li[1], Yangyang Liu[2], Zixiao Jiang[2], Haolin Wu[3]*, and Jing Lin[1]*

[1]Preparation Department, Hainan Fifth People's Hospital, Haikou, Hainan, China

[2]Hainan Key Laboratory of Protection and Utilization of Medicinal Plant Resources, Hainan Branch Institute of Medicinal Plant Development, Chinese Academy of Medical Sciences, Haikou, Hainan, China

[3]International Center for Aging and Cancer, Hainan Medical University, Haikou, Hainan, China

Abstract

Introduction: Ai Da Lotion is widely used for eczema in the clinic; however, its active ingredients and molecular mechanism remain unclear.

Objective: We set out to define the molecular basis for how Ai Da Lotion—a compound traditional Chinese medicine preparation—acts to treat eczema, with the goal of generating sound scientific support for its clinical use and modern translational development.

Methods: In this study, we combined ultra high-performance liquid chromatography–quadrupole time-of-flight mass spectrometry profiling with network pharmacology and molecular docking to identify the formula's bioactive constituents and key targets, then validated these findings in keratinocyte-based models of eczema.

Results: Chemical profiling identified 889 constituents, and physicochemical screening narrowed these to 42 candidate active compounds. Target network analysis uncovered 37 core nodes, with Janus kinase 1 (JAK1) and signal transducer and activator of transcription 3 (STAT3) emerging as the dominant regulatory pair. Two lead compounds—8-deoxylactucin and 6β-hydroxymethandrostenolone—bound JAK1 and STAT3 with high affinity (binding energy <–7.6 kcal/mol). Functionally, Ai Da Lotion promoted keratinocyte migration, attenuated oxidative stress, stabilized mitochondrial membrane potential, and suppressed Caspase-3–mediated apoptosis. These protective effects were recapitulated upon JAK1/STAT3 overexpression and blocked by selective pathway inhibition, indicating that the formula works primarily through JAK1/STAT3 modulation.

Conclusion: Our results provide a mechanistic basis for Ai Da Lotion and illustrate a practical strategy for dissecting the pharmacology of complex herbal dermatological preparations.

Keywords: Ai Da Lotion; Eczema; Ultra high-performance liquid chromatography–quadrupole time-of-flight mass spectrometry; Network pharmacology; Molecular docking; Janus kinase 1/signal transducer and activator of transcription 3 signaling pathway

***Corresponding authors:**
Haolin Wu
(2504935557@qq.com);
Jing Lin
(13876300091@163.com)

Citation: Li Y, Liu Y, Jiang Z, Wu H, Lin J. Ai Da Lotion improves eczema lesions via modulation of the JAK1/STAT3 pathway and regulation of apoptosis and oxidative stress. *Eurasian J Med Oncol.*
doi: 10.36922/EJMO026090094

Received: February 23, 2026

Revised: May 14, 2026

Accepted: June 1, 2026

Published online: July 8, 2026

1. Introduction

Eczema is one of the most common chronic inflammatory skin diseases worldwide, taking a heavy clinical and socioeconomic toll on affected individuals and healthcare systems. Eczema has a greater impact on infants and young children, and well-established epidemiological trends highlight markedly higher disease prevalence in Asian and Black communities relative to Caucasian populations.[1,2] Epidemiological estimates suggest this condition affects roughly 30% of children and 10% of adults in developed regions.

In China, the adult prevalence has been reported at 7.5%.[3,4] While not life-threatening, eczema follows a chronic, often lifelong course that imposes far-reaching burdens across social, emotional, physical, and socioeconomic dimensions. A growing body of evidence indicates that its disabling symptoms—most notably pruritus and pain—can severely affect sleep architecture, psychological health, cognitive performance, and daily functioning.[5-10]

Beyond direct morbidity, those affected carry a significantly elevated risk of a wide array of psychiatric and medical comorbidities, among them alopecia areata, major depressive disorder, attention-deficit/hyperactivity disorder, osteoporosis, anemia, obesity, and various cardiovascular disorders.[11-14] Its complex pathophysiology arises from the dynamic interplay of genetic susceptibility, impaired skin barrier function, dysregulated cellular immune responses, and environmental and lifestyle factors.[15,16] A systematic review of 800 studies focusing on traditional Chinese medicine showed that, across 435 clinical investigations evaluating herbal lotions for chronic eczema, the reported therapeutic response rates ranged from 81.44% to 100%, with a pooled mean effectiveness of 94.99%.[17-19]

Traditional Chinese Medicine (TCM) etiological models consider that eczema arises primarily from constitutional weakness, compounded by insufficient Zheng Qi, impaired transformative function of the spleen, and subsequent invasion by wind–damp–heat pathogenic factors.[20] Pathophysiologically, acute eczema is typified by damp-heat retention, whereas the subacute phase centers on spleen deficiency with damp accumulation, and chronic progression is characterized by *yin*-blood depletion that stirs endogenous wind and dryness.[20,21] This clinical framework defines four core syndromic patterns in eczema: (i) damp-heat, (ii) spleen deficiency with damp retention, (iii) blood deficiency with wind-dryness, and (iv) yin deficiency with blood dryness.[21,22]

While targeting the underlying etiologies remains central to management, topical therapy stands as a key therapeutic pillar, requiring careful selection of minimally irritating, low-sensitizing external preparations. In 2021, our institutional research and development team created Ai Da Lotion, which was subsequently approved as a hospital preparation (License No.: Qiongyao Zhizibei Z2021000300). This refined formulation integrates eight medicinal herbs: (i) Artemisiae argyi folium (mugwort leaf), (ii) Rhei radix et rhizoma (rhubarb), (iii) Senecionis scandentis herba (climbing groundsel), (iv) Sophorae flavescentis radix (light-yellow sophora), (v) Kochiae fructus (broom cypress), (vi) Smilacis glabrae rhizoma (glabrous greenbrier), (vii) Dictamni cortex (densefruit pittany), and (viii) Chrysanthemi indici flos (wild chrysanthemum). With its rational herb compatibility and notable clinical effectiveness, this formulation represents a well-optimized herbal external remedy.

While Ai Da Lotion has demonstrated consistent clinical efficacy over time, the complex chemical nature of multi-herbal TCM preparations has limited definitive characterization of its bioactive components, therapeutic targets, and pharmacodynamic mechanisms of action. By using an integrated network pharmacology and molecular docking strategy focused on its key bioactive constituents, this study aims to clarify the molecular mechanisms by which the lotion acts against eczema. Through holistic network analysis, we characterized systems-level modulation of disease-relevant targets and identified cryptic target-pathway interactions. These findings provide mechanistic and empirical support for the evidence-based use of Ai Da Lotion in eczema therapy, advancing novel therapeutic frameworks for TCM-derived dermatological interventions.

2. Materials and methods

2.1. Instruments

Ultra high-performance liquid chromatograph (LC-30A; Shimadzu, Japan), quadrupole time-of-flight mass spectrometer (TripleTOF 6600+; SCIEX, USA), refrigerated centrifuge (5424R; Eppendorf, Germany), thermomixer (MU-G02-0448; Hangzhou Miou Instruments Co., Ltd., China), analytical balance (readability: 0.01 mg; MS105DM; Mettler-Toledo International Inc., USA), centrifugal evaporator (CentriVap; LABCONCO, USA), vortex mixer (VORTEX-5; Kylin-Bell Lab Instruments Co., Ltd., China), and ultrasonic cleaner (KQ5200E; Kunshan Ultrasonic Instruments Co., Ltd., China) were used in this study.

2.2. Materials and reagents

Artemisiae argyi folium (lot no. 2408101), Rhei radix et

rhizoma (lot no. 2407101), Senecionis scandentis herba (lot no. 2406102), Sophorae flavescentis radix (lot no. 2406101), Kochiae fructus (lot no. 2407101), Smilacis glabrae rhizoma (lot no. 2405101), Dictamni cortex (lot no. 2408101), and Chrysanthemi indici flos (lot no. 2406101) were purchased from Hainan Xinxing Shenrong Pharmaceutical Co., Ltd. (China).

For chromatographic and experimental analyses, high-performance liquid chromatography (HPLC)-grade methanol (Merck, Germany), HPLC-grade acetonitrile (Merck, Germany), HPLC-grade formic acid (Aladdin, China), and anhydrous ethanol (Xilong Chemical Co., Ltd., China) were used.

2.3. Chemical profiling of Ai Da Lotion

2.3.1. Sample preparation

A 0.5 mL portion of the medicinal solution was pipetted into a 1.5 mL microcentrifuge tube, vortexed vigorously for 15 min, and then centrifuged at 12,000 rpm at 4 °C for 3 min. The resulting supernatant was carefully collected, passed through a 0.22 μm membrane filter, and transferred to an autosampler vial prior to liquid chromatography–tandem mass spectrometry analysis.

2.3.2. Chromatographic and mass spectrometric conditions

Chromatographic separation was carried out on a Waters ACQUITY UPLC HSS T3 column (1.8 μm; 2.1 mm × 100 mm) maintained at 40°C. The mobile phase was composed of 0.1% formic acid in water (A) and 0.1% formic acid in acetonitrile (B), delivered at a flow rate of 0.4 mL/min, with an injection volume of 4 μL. Gradient elution was performed as follows, with mass spectrometric parameters detailed in Table 1: starting at 95% A, linearly decreased to 35% A at 5 min, then decreased further to 1% A at 6 min and held for 1.5 min, then re-equilibrated to 95% A at 7.6 min for the remainder of the 10-min run.

Table 1. Mass spectrometry conditions

Parameter name	ESI+	ESI−
Duration (min)	10	10
Ionspray voltage (V)	5,000	−4,000
Temperature (°C)	550	550
Ion source gas 1 (psi)	50	50
Ion source gas 2 (psi)	60	60
Curtain gas (psi)	35	35
Declustering potential (v)	60	−60
MS1 collision energy (v)	10	−10
MS2 collision energy (v)	30	−30
Collision energy spread(v)	15	15
MS1 TOF masses (da)	50–1,250	50–1,250
MS2 TOF masses (da)	25–1,250	25–1,250

Abbreviations: ESI: Electrospray ionization; MS: Mass spectrometry; TOF: Time-of-flight.

2.4. Chemical constituent screening and target prediction

The constituents identified in Section 2.3 were curated and annotated using PubChem (https://pubchem.ncbi.nlm.nih.gov/) to obtain canonical SMILES representations. Subsequent physicochemical filtering was performed with SwissADME (https://www.swissadme.ch/) under stringent criteria (iLogP ≤ 5, hydrogen-bond donors ≤ 5, hydrogen-bond acceptors ≤ 10, and oral bioavailability ≥30%), followed by verification of Lipinski's rule compliance. Final compound selection prioritized those with high gastrointestinal absorption and favorable lead-likeness profiles, thus defining the bioactive component library of Ai Da Lotion.

2.5. Eczema-associated target dataset curation

To mitigate database-specific gaps in coverage, we queried two complementary repositories—GeneCards (https://www.genecards.org/) and DisGeNET (https://www.disgenet.org/)—using "eczema" as the search term. Only targets with a relevance score of ≥2 were retained, ensuring both clinical relevance and data reliability.

2.6. Protein–protein interaction network construction

Overlapping targets between the bioactive constituents of Ai Da Lotion and eczema-associated genes were identified through intersection analysis, defining the therapeutic target profile. This dataset was uploaded to STRING (https://cn.string-db.org/) to construct a protein–protein interaction network, with *Homo sapiens* specified as the reference organism and an interaction confidence cutoff of 0.7. Topological analysis and network visualization were conducted using Cytoscape version 3.9.1 (Cytoscape Team, USA).

2.7. Multi-hierarchical network modeling

A multi-tiered "component–target–pathway" network was constructed in Cytoscape version 3.9.1 by integrating

the core bioactive constituents, key therapeutic targets, and eczema-associated pathways. For network topology, circular nodes represented therapeutic targets, diamond nodes denoted bioactive compounds, and triangular nodes symbolized the composite formula—collectively illustrating the systems-level modulation of eczema pathophysiology.

2.8. Functional enrichment analysis

The identified target set was subjected to Gene Ontology (GO) and Kyoto Encyclopedia of Genes and Genomes (KEGG) pathway enrichment analyses using Metascape (https://metascape.org/) and DAVID (https://david.ncifcrf.gov/). GO analysis covered three core ontological domains—biological processes, cellular components, and molecular functions—and elucidated the mechanistic basis of the therapeutic effects of the composite formula.

2.9. Molecular docking validation

Key bioactive constituents and hub targets were prioritized based on network centrality metrics for molecular docking validation. Ligand structures (in SDF format) and protein coordinates (in PDB format) were retrieved from PubChem and RCSB PDB (https://www.rcsb.org/), respectively. AutoDock (version 1.2.7, Oleg Trott, USA) was used to perform docking simulations, with PyMOL (version 3.1.8, Warren Lyford DeLano, USA) employed for interactive complex visualization. A binding energy cutoff of below −1.4 kcal/mol was defined to indicate high-affinity interactions, serving as the benchmark for pharmacological validation.

2.10. Skin cell scratch assay

Skin-derived cells (Procell, China) were seeded into 6-well plates at a density of 1×10^5 and cultured in Dulbecco's Modified Eagle Medium (Gibco, USA) supplemented with 10% fetal bovine serum (Gibco, USA) and antibiotics (Gibco, USA) at 37 °C in a 5% CO_2 incubator until reaching 90–100% confluency and forming a continuous monolayer to mimic skin barrier integrity.

Prior to scratch creation, experimental interventions were performed as designed—including lipopolysaccharide (LPS)-induced inflammatory stimulation, Ai Da Lotion treatment, or Janus kinase 1 (JAK1)/signal transducer and activator of transcription 3 (STAT3) overexpression—and the cells were incubated for the specified duration.[23,24] A sterile 200 μL pipette tip was used to create uniform linear scratches vertically across the cell monolayer. Consistent pressure was applied to maintain uniform scratch widths across all wells. The plates were immediately washed 2–3 times with pre-warmed phosphate-buffered saline (PBS; Thermo Fisher Scientific, USA) to remove detached cells and debris, then replenished with serum-free Dulbecco's Modified Eagle Medium or medium containing the corresponding interventions. Three to four fixed observation points were marked per scratch using plate grid lines to ensure imaging of the same areas at different time points.

The plates were incubated continuously, and representative images of the marked areas were captured at 0 h, 24 h, and 48 h using an inverted microscope (Olympus Corporation, Japan; 100× or 200× magnification). Scratch closure rates were analyzed with image analysis software (ImageJ, version 1.54f, National Institutes of Health, USA). The scratch width was measured at five random positions per observation point, and the average width was calculated for each time point. The closure rate was determined using the following formula:

$$Closure\ rate = \frac{0\ h\ average\ width - target\ time\ point\ average\ width}{0\ h\ average\ width} \times 100\% \quad (1)$$

The following experimental considerations were taken into account during the assay:

(i) Sterile technique was maintained throughout to prevent contamination.
(ii) Excessive washing was avoided to prevent additional cell detachment.
(iii) Consistent scratch direction and force were ensured for inter-group comparability.
(iv) At least three replicate wells were included per group to ensure statistical reliability.
(v) For skin-derived cells, medium composition was adjusted as needed (e.g., by supplementing the medium with keratinocyte growth factor for keratinocytes) to maintain cell viability during the assay.
(vi) Prolonged serum starvation was avoided because it can induce abnormal cellular stress.

2.11. Establishment of a mouse model of skin inflammatory injury

Specific-pathogen-free BALB/c mice (6–8 weeks old; n = 24) were acclimatized for seven days under standard conditions (22 ± 2 °C, 12-h light/dark cycle). The dorsal hair was carefully shaved to expose an intact skin area of approximately 2×2 cm^2. An acute inflammatory skin lesion model was established by daily topical application of LPS (*Escherichia coli* O111:B4; Sigma-Aldrich, USA; 50 μg LPS dissolved in 100 μL sterile PBS) onto the shaved skin once daily for five consecutive days. The solution was gently and evenly distributed over the designated area and allowed to absorb.

2.12. Hematoxylin and eosin staining and immunohistochemical staining experimental methods

The tissue was fixed in 4% paraformaldehyde and processed into paraffin-embedded sections with a thickness of 4 μm. For hematoxylin and eosin (H&E) staining, the sections were stained with H&E after standard dehydration, and epidermal thickness and inflammatory changes were evaluated under an optical microscope.

For immunohistochemical staining, the sections underwent heat-mediated antigen retrieval (using citrate buffer, pH 6.0), were neutralized with 3% hydrogen peroxide, and blocked using 3% bovine serum albumin (BSA; Sigma, USA). The sections were incubated overnight at 4 °C with a primary antibody against caspase-3 (1:200; catalog no: 9H19L2, Thermo Fisher, USA), and then incubated at room temperature for 1 h with a horseradish peroxidase-conjugated secondary antibody (1:500; 725169ES10, Yeasen, China). The immunoreactivity was visualized with 3,3'-diaminobenzidine and counterstained with hematoxylin, followed by microscopic examination.

2.13. Immunofluorescence

For the simultaneous detection of oxidative stress (reactive oxygen species [ROS]), cell proliferation (EdU), apoptosis (cleaved caspase-3), and mitochondrial function (JC-1) in *in vitro* eczema models, an integrated immunofluorescence assay was performed as follows: target cells were first seeded into 6-well plates containing coverslips at a cell density of 1×10^4 cells/well. When cell confluency reached 60–80%, experimental interventions (e.g., LPS induction, Ai Da Lotion treatment, JAK1/STAT3 overexpression) were conducted, followed by the addition of 10 μM EdU working solution (40276ES60, Yeasen, China) to the medium and incubation at 37 °C for 2 h. The medium was aspirated, and cells were washed three times with PBS (5 min per wash), fixed with 4% paraformaldehyde at room temperature for 15 min, and permeabilized with 0.1% Triton X-100 (Yeasen, China) for 10 min. After an additional three PBS washes, an EdU reaction cocktail (prepared according to the kit instructions) was added, and cells were incubated in the dark for 30 min, followed by three further PBS washes.

Next, cells were incubated with 10 μM 2',7'-dichlorodihydrofluorescein diacetate probe (Yeasen, China; diluted in serum-free Dulbecco's Modified Eagle Medium medium) at 37 °C in the dark for 20 min, washed three times with serum-free Dulbecco's Modified Eagle Medium medium, and subsequently incubated with 5 μM JC-1 working solution (Yeasen, China) at 37 °C in the dark for 20 min. After two washes with pre-warmed PBS, cells were re-fixed with 4% paraformaldehyde for 10 min. Following three PBS washes, cells were blocked with 5% BSA at room temperature for 1 h. The blocking solution was aspirated, and a diluted cleaved caspase-3 primary antibody (1:100–1:500 in 5% BSA; Asp175, CST, USA) was added for overnight incubation at 4 °C.

On the following day, cells were rewarmed at room temperature for 30 min, washed three times with PBS, and incubated with an Alexa Fluor 647-labeled secondary antibody (1:500–1:1,000; A-21245, Thermo Fisher, USA) in the dark for 1 h, followed by three additional PBS washes. Finally, nuclei were stained with 1:1,000 diluted 4',6-diamidino-2-phenylindole in the dark for 5 min.

After three final PBS washes, coverslips (cell side down) were mounted onto glass slides using anti-fluorescence quenching medium (while avoiding air bubbles), air-dried at room temperature, and stored in the dark at 4 °C for imaging within 24–48 h.

The sequential staining order was strictly followed to preserve probe activity. All fluorescence-based steps were performed in the dark to prevent photobleaching. Sufficient washing was ensured to minimize background fluorescence. Non-overlapping fluorescence channels were assigned for multiplex detection, with ROS visualized in the fluorescein isothiocyanate channel, EdU in the tetramethylrhodamine isothiocyanate channel, cleaved caspase-3 in the far-red channel, JC-1 detected in both fluorescein isothiocyanate (monomer) and tetramethylrhodamine isothiocyanate (aggregate) channels, and nuclei counterstained with 4',6-diamidino-2-phenylindole.[25-28]

2.14. Statistical analysis

All experiments were performed in triplicate with at least three independent biological replicates. Data are presented as mean ± standard error of the mean or mean ± standard deviation, as appropriate. Statistical analyses were carried out using GraphPad Prism version 9.0 software (GraphPad, USA).

3. Results

3.1. Phytochemical profiling and target spectrum construction of Ai Da Lotion

Qualitative analysis using ultra high-performance liquid chromatography–quadrupole time-of-flight mass spectrometry identified a total of 889 constituents in Ai Da Lotion. These compounds represented diverse chemical classes, including 532 amino acids and derivatives, 62 benzene analogs, 8 alcohol/amine derivatives, 12 phenolic acids, 5 glycerophospholipids, 2 glycerides, 9 nucleotides and analogs, 24 flavonoids, 2 quinones, 10 lignans/coumarins, 83 miscellaneous compounds, 32 alkaloids, 11 terpenoids, 48 organic acids, 20 heterocyclic compounds, 2 steroids, 3 fatty acyls, and 24 lipid species (Figure 1).

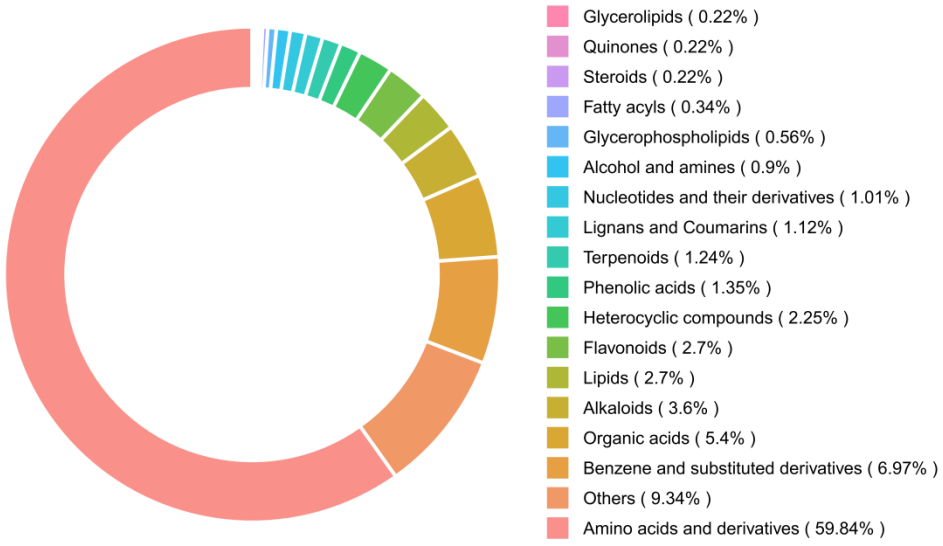

Figure 1. Chemical composition distribution of Ai Da Lotion

Table 2. Effective active ingredients of Ai Da Lotion

No.	Compound	Primary classification of substances	Secondary classification of substances	Molecular weight (g/mol)
ADXJ001	Acetylvalerenolic acid	Terpene	Sesquiterpenes	292.37
ADXJ002	L-histidine β-naphthylamide	Alkaloid	Indole alkaloid	280.32
ADXJ003	Thiamine	Other categories	Vitamin	265.35
ADXJ004	Kahweol	Heterocyclic compound	Heterocyclic compound	314.42
ADXJ005	8-deoxylactucin	Terpene	Sesquiterpenes	260.29
ADXJ006	(S)-Scoulerine	Alkaloid	Isoquinoline alkaloids	327.37
ADXJ007	(9bR)-2,6-diacetyl-7,9-dihydroxy-8,9b-dimethyldibenzo[b,d]furan-1,3(2H,9bH)-dione	Benzene and its derivatives	Benzene and its derivatives	344.32
ADXJ008	Maesopsin	Benzene and its derivatives	Benzene and its derivatives	288.25
ADXJ009	N-(3-indolylacetyl)-L-isoleucine	Amino acids and their derivatives	Amino acids and their derivatives	288.34
ADXJ010	Physostigmine	Heterocyclic compound	Heterocyclic compound	275.35
ADXJ011	Capillarisin	Other categories	Chromones	316.26
ADXJ012	N-[[4-[(pyridin-2-ylamino)methyl] phenyl]methyl]pyridin-2-amine	Benzene and its derivatives	Benzene and its derivatives	290.36
ADXJ013	3-hydroxyquinidine	Alkaloid	Alkaloid	340.42
ADXJ014	Cocaethylene	Other categories	Lactone compounds	317.38
ADXJ015	Convolamine	Benzene and its derivatives	Benzene and its derivatives	305.37
ADXJ016	Seneciphylline	Alkaloid	Pyrrole alkaloids	333.38
ADXJ017	Neopine	Benzene and its derivatives	Benzene and its derivatives	299.36
ADXJ018	L-phenylalanyl-L-valine	Amino acids and their derivatives	Amino acids and their derivatives	264.32

(*Cont'd...*)

Table 2. (*Continued*)

No.	Compound	Primary classification of substances	Secondary classification of substances	Molecular weight (g/mol)
ADXJ019	Aegeline	Alkaloid	Phenamine	297.35
ADXJ020	2',4-dihydroxy-4',6'-dimethoxychalcone	Flavone	Chalcone	300.31
ADXJ021	Ascochitine	Benzene and its derivatives	Benzene and its derivatives	276.28
ADXJ022	1-(2,6-Dihydroxy-4-methoxyphenyl)-3-(4-methoxyphenyl)propan-1-one	Other categories	Ketone compounds	302.32
ADXJ023	6β-Hydroxymethandrostenolone	Other categories	Ketone compounds	316.43
ADXJ024	(2R,3S)-Methyl 3-benzamido-2-hydroxy-3-phenylpropanoate	Benzene and its derivatives	Benzene and its derivatives	299.32
ADXJ025	Bracteatin	Other categories	Ketone compounds	302.24
ADXJ026	Cephalotaxine	Alkaloid	Isoquinoline alkaloids	315.36
ADXJ027	3,7,4'-Trihydroxyflavone	Flavone	Flavone	270.24
ADXJ028	Micromelin	Other categories	Lactone compounds	288.25
ADXJ029	Abscisic acid	Organic acid	Organic acid	264.32
ADXJ030	(4Ar,6aS,9aR)-1,8,8-trimethyl-2-oxo-1,4,4a,6a,7,9-hexahydropentaleno[1,6a-c]pyran-5-carboxylic acid	Terpene	Sesquiterpenes	264.32
ADXJ031	5,7,8-Trimethoxy-3-(4-methoxyphenyl)chromen-4-one	Benzene and its derivatives	Benzene and its derivatives	342.34
ADXJ032	5-Hydroxy-2,8-dimethyl-6,7,8,9-tetrahydropyrano[3,2-h][1]benzoxepin-4-one	Benzene and its derivatives	Benzene and its derivatives	260.29
ADXJ033	Senecionine	Other categories	Lactone compounds	335.39
ADXJ034	Thebaine	Alkaloid	Isoquinoline alkaloids	311.37
ADXJ035	1,4-Dibenzylpiperazine	Benzene and its derivatives	Benzene and its derivatives	266.38
ADXJ036	Eucatropine	Heterocyclic compound	Heterocyclic compound	291.39
ADXJ037	12-hydroxy-podocarpa-8,11,13-trien-16-oic acid	Terpene	Diterpene	274.35
ADXJ038	Methyl (1S,2R,3S,5S)-3-benzoyloxy-8-methyl-8-azabicyclo[3.2.1]octane-2-carboxylate	Benzene and its derivatives	Benzene and its derivatives	303.35
ADXJ039	Genistein, 8-methyl	Other categories	Ketone compounds	284.26
ADXJ040	3,4,6-trimethoxy-5-oxo-8-benzo[7]annulenecarboxylic acid methyl ester	Benzene and its derivatives	Benzene and its derivatives	304.29
ADXJ041	Azacyclonol	Benzene and its derivatives	Benzene and its derivatives	267.37
ADXJ042	N-Acetylvanilalanine	Amino acids and their derivatives	Amino acids and their derivatives	253.25

Applying Lipinski's rule of five with constraints (with the following criteria: iLogP ≤ 5, hydrogen-bond donors ≤ 5, hydrogen-bond acceptors ≤ 10, and oral bioavailability ≥ 30%), 42 active compounds were identified from Ai Da Lotion for eczema treatment (Table 2), comprising 3 amino acids and derivatives, 13 benzene derivatives, 2 flavonoids, 7 alkaloids, 4 terpenoids, 3 heterocyclic compounds, and 9 miscellaneous compounds.

3.2. Protein–protein interaction network construction and topological analysis

Database interrogation with "ECZEMA" retrieved 46 disease-associated genes post-filtering. By comparing the 42 active compounds with eczema-related genes, 37 overlapping targets were identified. STRING-based protein–protein interaction network construction generated a topology encompassing 37 nodes, 89 edges, and an average degree centrality of 4.81—with nine nodes persisted as isolated singletons. Enrichment analysis demonstrated robust biological connectivity ($p < 1 \times 10^{-16}$) (Figure 2). The network resolved into two distinct submodules: a triadic cluster (STS–DHCR7–CYP24A1) and a dyadic pair (TRPV1–TACR1). Centrality ranking by degree identified *STAT1*, *TNF*, *STAT3*, *IL2*, *PIK3R1*, *SYK*, *PTPRC*, *TYK2*, *JAK1*, and *JAK3* as the top ten core targets (Table 3).

3.3. Functional enrichment analysis

Enrichment analysis of the 37 therapeutic targets revealed significant involvement across multiple biological processes, including leukocyte activation ($p = 4.57 \times 10^{-23}$), regulation of cytokine production ($p = 2.57 \times 10^{-19}$), inflammatory response ($p = 2.24 \times 10^{-18}$), regulation of lymphocyte proliferation ($p = 7.08 \times 10^{-17}$), and response to hormones ($p = 3.31 \times 10^{-16}$).

Table 3. Top 10 target information

Gene	MCC	DMNC	MNC
STAT1	1,944	0.46666	16
TNF	380	0.37055	15
STAT3	1,902	0.50675	14
IL2	1,026	0.49759	12
PIK3R1	876	0.45814	11
SYK	210	0.49882	10
PTPRC	72	0.40573	9
TYK2	1,704	0.69213	9
JAK1	1,680	0.66826	9
JAK3	1,566	0.62053	9

Abbreviations: DMNC: Density of maximum neighborhood component; MCC: Maximal clique centrality; MNC: Maximum neighborhood component.

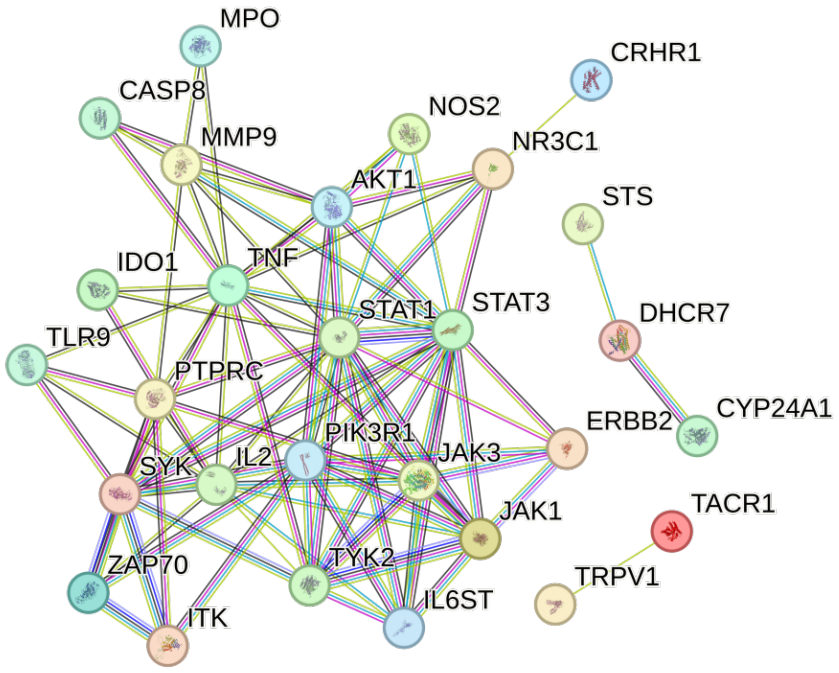

Figure 2. Protein–protein interaction network of 37 intersecting target genes

Analysis of cellular component terms showed significant localization to the membrane periphery ($p = 1.41 \times 10^{-8}$), external side of the plasma membrane ($p = 8.91 \times 10^{-6}$), plasma membrane protein complexes ($p = 2.63 \times 10^{-5}$), dendrites ($p = 1.00 \times 10^{-4}$), and perinuclear cytoplasmic regions ($p = 2.51 \times 10^{-4}$).

The most significantly enriched molecular functions included cytokine receptor binding ($p = 3.55 \times 10^{-16}$), non-membrane-spanning tyrosine kinase activity ($p = 1.70 \times 10^{-11}$), phosphoprotein binding ($p = 1.07 \times 10^{-7}$), scaffold protein binding ($p = 1.62 \times 10^{-6}$), and protein kinase binding ($p = 1.95 \times 10^{-6}$). KEGG pathway analysis identified five significantly enriched pathways: Measles ($p = 9.12 \times 10^{-16}$), Chagas disease ($p = 8.91 \times 10^{-6}$), primary immunodeficiency ($p = 2.63 \times 10^{-5}$), microRNAs in cancer ($p = 1.00 \times 10^{-4}$), and neuroactive ligand–receptor interaction ($p = 2.51 \times 10^{-4}$) (Figure 3).

3.4. Multi-hierarchical network construction

A component–target–pathway network for Ai Da Lotion was built and mapped in Cytoscape version 3.9.1, integrating active constituents, therapeutic targets, and eczema-associated genes. Figure 4 illustrates the target profile linked to each individual constituent.

3.5. Molecular docking validation

In this study, JAK1 and STAT3 were selected as central docking targets based on their connectivity and centrality metrics, with 8-deoxylactucin (ADXJ005) and 6β-hydroxymethandrostenolone (ADXJ023) chosen as core ligands.

For docking simulations, the crystal structures of JAK1 (PDB: 6ggh) and STAT3 (PDB: 6njs) were used. All protein–ligand complexes exhibited binding energy values lower than −1.4 kcal/mol, suggesting favorable binding affinity. Collectively, these findings indicate that the bioactive constituents of Ai Da Lotion can effectively bind to core therapeutic targets (Table 4; Figure 5).

Table 4. Molecular docking information table

Active ingredients	Target of rapamycin	Binding energy (kcal/mol)
8-deoxylactucin (ADXJ005)	JAK1	−5.49
	STAT3	−6.29
6β-hydroxymethandrostenolone (ADXJ023)	JAK1	−7.61
	STAT3	−8.01

Abbreviations: JAK1: Janus kinase 1; STAT3: Signal transducer and activator of transcription 3.

3.6. Ai Da Lotion improves scratch injury in eczema models via the JAK1/STAT3 pathway

Scratch wound healing assay was performed to assess cell

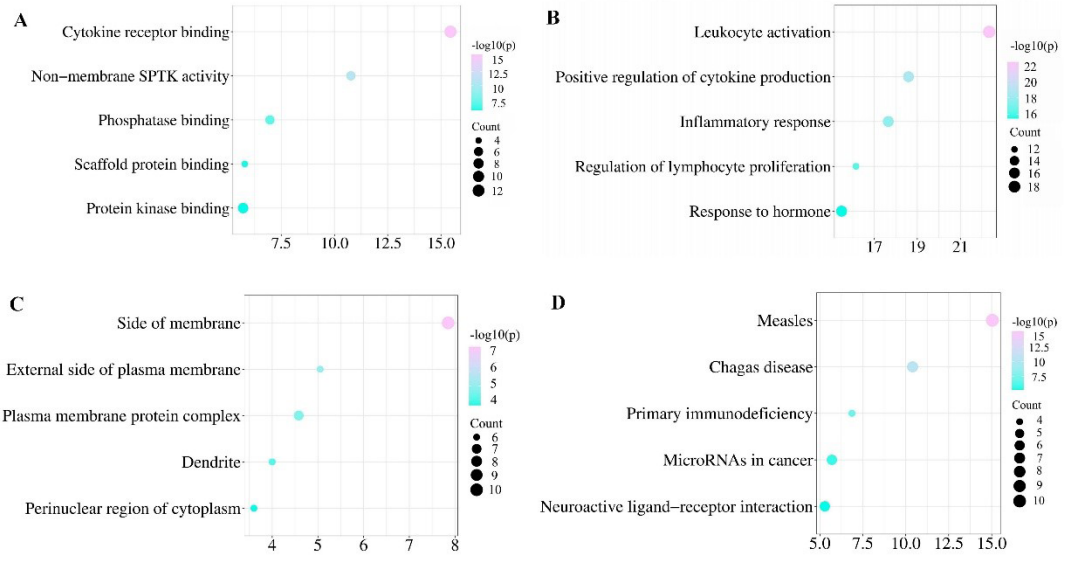

Figure 3. Gene Ontology functional enrichment and Kyoto Encyclopedia of Genes and Genomes pathway analysis of Ai Da Lotion: (A) Molecular function, (B) biological process, (C) cellular component, and (D) Kyoto Encyclopedia of Genes and Genomes signaling pathways.

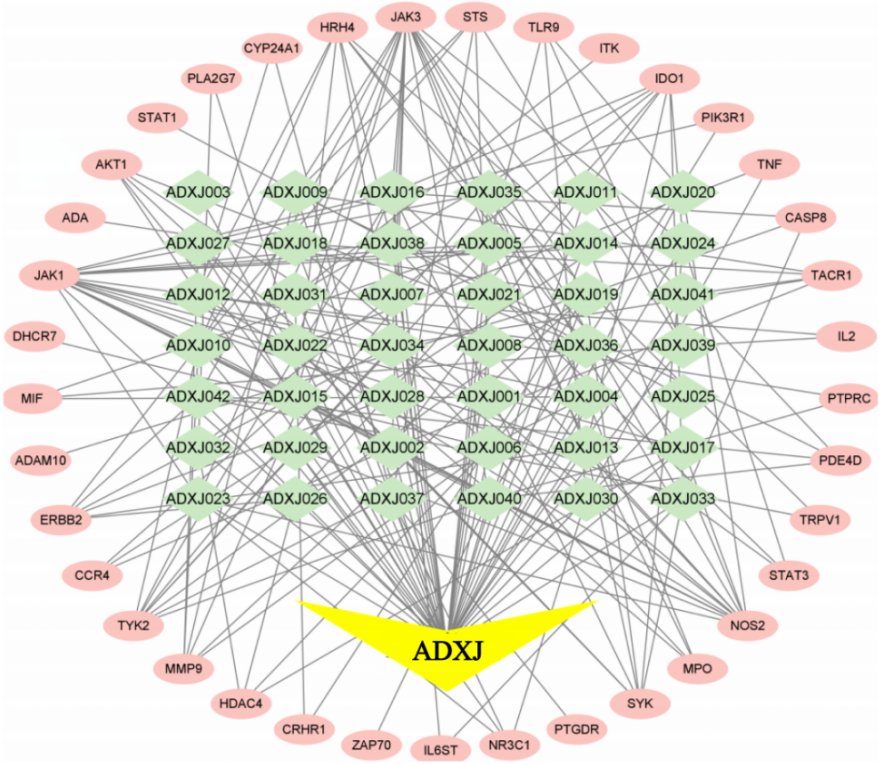

Figure 4. Component–target–pathway network of Ai Da Lotion. Pink circular nodes represent anti-eczema functional targets, green diamond nodes correspond to bioactive components, and edges depict regulatory interactions.

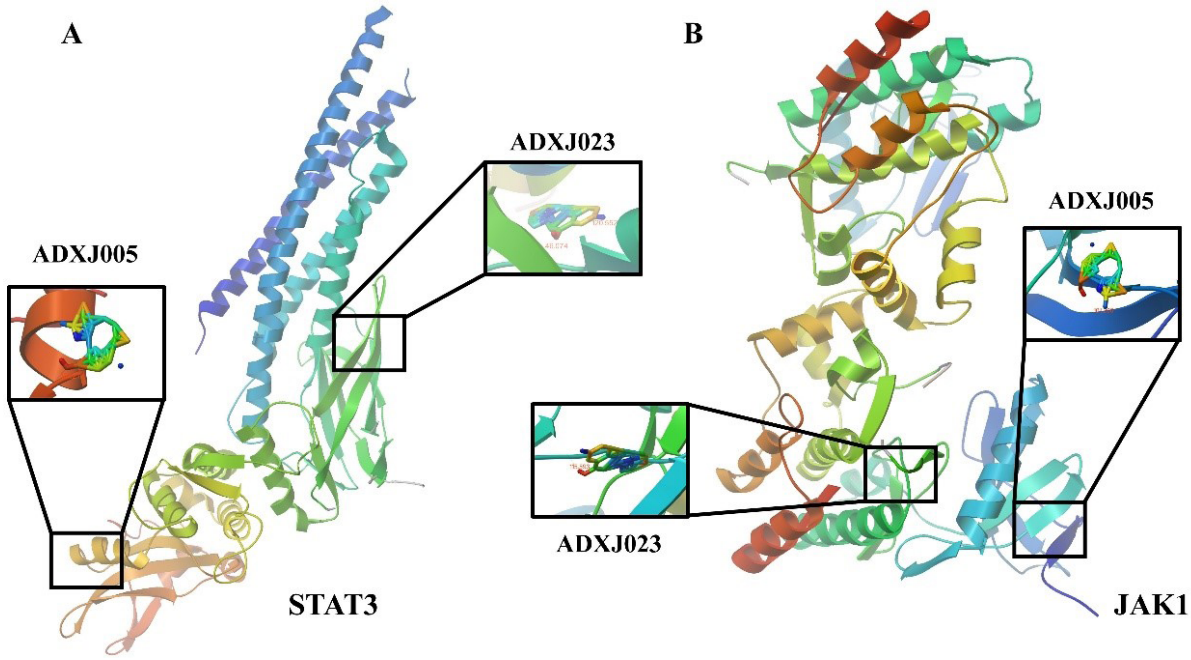

Figure 5. Molecular docking results: (A) STAT3 with ADXJ005 and ADXJ023 and (B) JAK1 with ADXJ005 and ADXJ023
Abbreviations: JAK1: Janus kinase 1; STAT3: Signal transducer and activator of transcription 3.

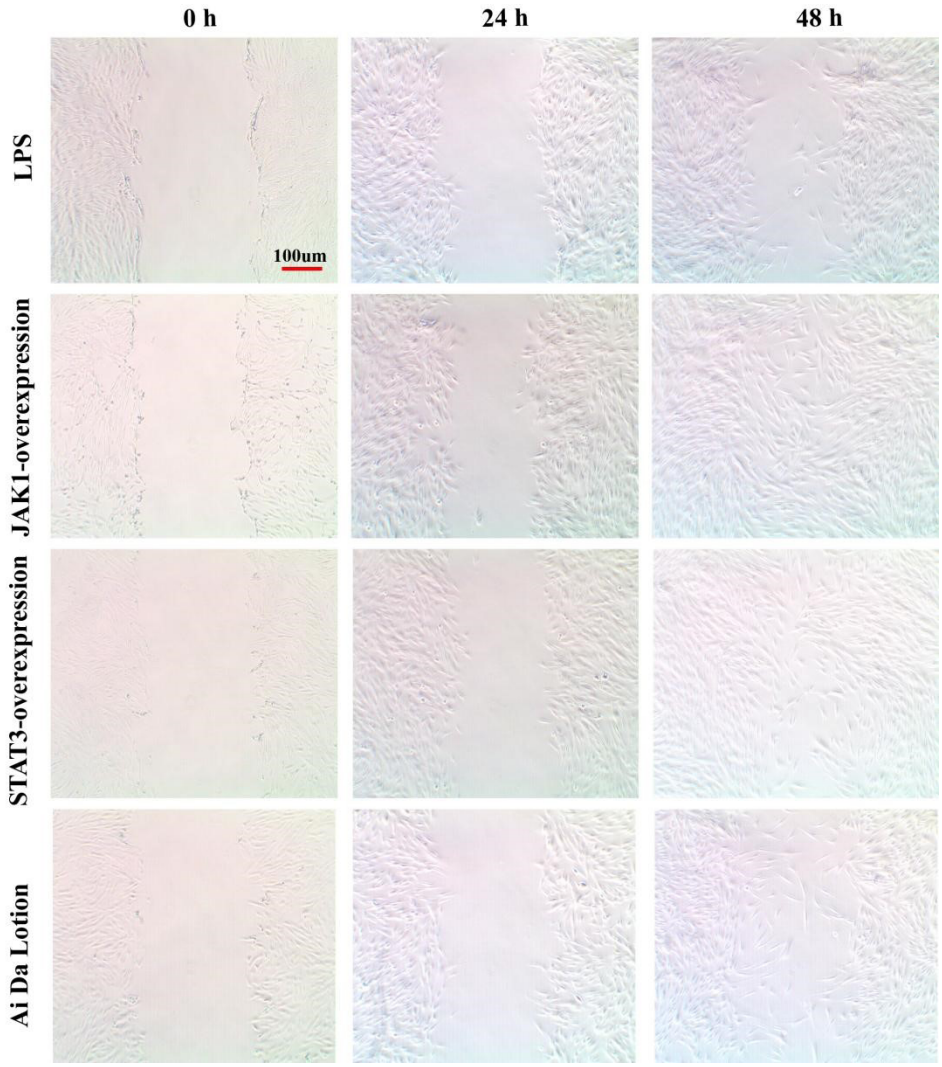

Figure 6. Representative images of scratch wound healing in the eczema model (LPS group) and treated groups (JAK1-overexpression, STAT3-overexpression, and Ai Da Lotion groups) at 0, 24, and 48 h (scale bar =100 μm; magnification = 10×)
Abbreviations: JAK1: Janus kinase 1; LPS: Lipopolysaccharide; STAT3: Signal transducer and activator of transcription 3.

migration under different treatments, with images captured at 0, 24, and 48 h (Figure 6). At the initial time point (0 h), all treatment groups—LPS, JAK1-overexpression, STAT3-overexpression, and Ai Da Lotion groups—showed uniform, well-defined wound gaps. There were no significant differences in gap width and cell distribution along the wound edges across these groups.

By 24 h, all groups exhibited cell migration toward the wound center, but the extent of gap closure differed markedly. The LPS group only showed partial narrowing of the wound gap, while the JAK1-overexpression, STAT3-overexpression, and Ai Da Lotion groups exhibited more extensive cell migration, resulting in reduced the residual wound area.

By 48 h, wound closure had progressed further: the LPS group still had a visible (though narrowed) gap, whereas the JAK1-overexpression, STAT3-overexpression, and Ai Da Lotion groups achieved near-complete wound closure, with dense cell populations filling the original gap region. Together, these findings showed that JAK1-overexpression, STAT3-overexpression, and Ai Da Lotion treatments enhance cell migratory capacity compared with LPS stimulation.

To further explore whether Ai Da Lotion protects skin cells from inflammatory damage via the JAK1/STAT3 signaling axis, EdU proliferation assay was conducted to examine cellular responses to inflammatory challenge (Figure 7). LPS exposure markedly reduce cell

proliferation, whereas treatment with Ai Da Lotion and modulation of the JAK1/STAT3 pathway both substantially alleviated LPS-induced cellular injury. These observations suggested that Ai Da Lotion mitigates eczema-associated inflammatory damage in skin cells by regulating the JAK1/STAT3 pathway.

Representative fluorescence images and quantitative analyses show that LPS stimulation leads to excessive ROS production—evident from intense green fluorescence—and mitochondrial dysfunction, which is characterized by reduced red JC-1 fluorescence and a low red/green ratio. In contrast, JAK1-overexpression group, STAT3-overexpression group, and Ai Da Lotion group markedly suppressed ROS generation and restored mitochondrial membrane potential (Figure 8). These molecular changes (reduced oxidative stress and preserved mitochondrial function) are consistent with the enhanced scratch wound healing observed following these interventions. Specifically, Ai Da Lotion, JAK1-overexpression, and STAT3-overexpression groups all significantly enhanced cell migration and scratch closure compared to the LPS group.

Taken together, these findings suggest that Ai Da Lotion could promote wound repair in the eczema model by modulating the JAK1/STAT3 signaling pathway, which in turn regulates oxidative stress and mitochondrial function.

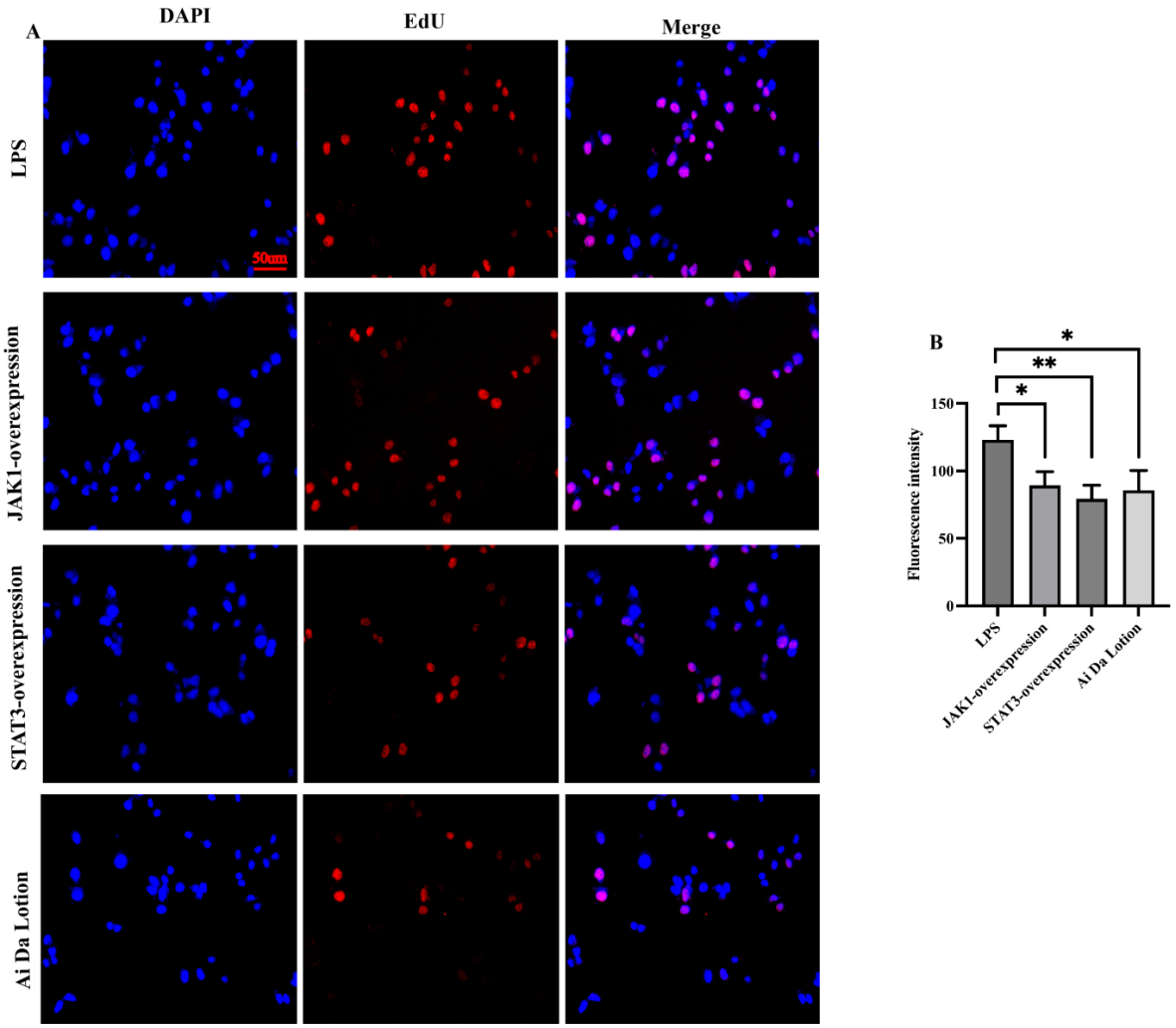

Figure 7. EdU staining of cell proliferation with representative fluorescence images and statistical analysis. (A) Representative fluorescence micrographs of EdU staining (red; proliferating cells) and DAPI nuclear counterstaining (blue; total cells), alongside merged images, are shown for the LPS-stimulated model group, JAK1-overexpression group, STAT3-overexpression group, and Ai Da Lotion-treated group (scale bar = 50 μm; magnification = 20×). (B) Quantification of EdU fluorescence intensity. *$p < 0.05$ and **$p < 0.01$ indicate statistically significant difference.
Abbreviations: DAPI: 4',6-diamidino-2-phenylindole; JAK1: Janus kinase 1; LPS: Lipopolysaccharide; STAT3: Signal transducer and activator of transcription 3.

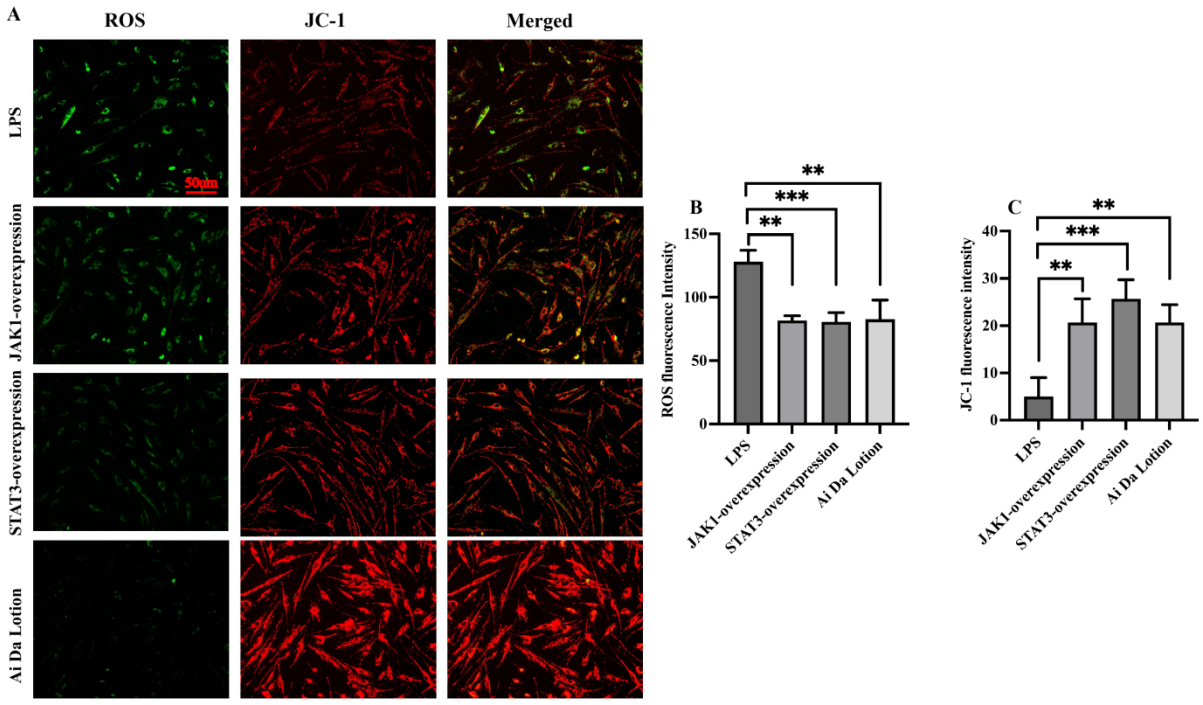

Figure 8. ROS production and mitochondrial membrane potential analysis in LPS-induced eczema *in vitro* models. (A) Representative fluorescence images of ROS staining (green) and JC-1 staining (red, high mitochondrial membrane potential; green, low mitochondrial membrane potential) in the LPS group, JAK1-overexpression group, STAT3-overexpression group, and Ai Da Lotion group (scale bar = 50 μm; magnification = 20×). (B) Quantitative analysis of ROS fluorescence intensity. (C) Quantitative analysis of JC-1 red/green fluorescence ratio. Data are presented as mean ± standard deviation (n = 3 independent experiments). Statistical significance is indicated as $^{*}p < 0.05$, $^{**}p < 0.01$, and $^{***}p < 0.001$ vs. LPS group.
Abbreviations: JAK1: Janus kinase 1; LPS: Lipopolysaccharide; ROS: Reactive oxygen species; STAT3: Signal transducer and activator of transcription 3.

Studies have shown that mitochondrial damage can lead to apoptosis. To further clarify whether cell apoptosis occurs in eczema cells and whether Ai Da Lotion can produce an improvement effect through the JAK1/STAT3 pathway, we conducted an immunofluorescence assay to detect the changes in the apoptosis marker caspase-3.

The immunofluorescence assay showed that LPS stimulation induces strong activation of caspase-3 and promotes apoptosis, while high expression of JAK1, high expression of STAT3, and treatment with Ai Da Lotion inhibit apoptosis in a dose-dependent manner. Among them, the inhibitory effect of Ai Da Lotion is the most significant (Figure 9). These findings suggest that Ai Da Lotion exerts an anti-apoptotic effect potentially through modulation of the JAK1/STAT3 signaling pathway, which supports its repair-promoting function in the eczema model.

Finally, to systematically evaluate the improvement effect of Ai Da Lotion on the inflammatory state of eczema and its possible mechanism, we used a mouse skin tissue injury model induced by LPS and administered corresponding intervention treatments based on this model. Then, we detected changes in relevant indicators through H&E staining and immunohistochemistry (Figure 10). The H&E staining results showed that the LPS model group exhibited a significantly disorganized epithelial structure, hyperkeratosis, and infiltration of inflammatory cells; the JAK1-overexpression, STAT3-overexpression, and Ai Da Lotion intervention groups showed a more complete epithelial structure, thicker stratum corneum, and significantly reduced inflammatory infiltration, with tissue morphology approaching physiological state.

The immunohistochemistry results showed that the LPS model group showed extensive positive expression of caspase-3 in the epithelial and dermal regions (dark brown staining), suggesting that LPS stimulation could significantly activate the apoptotic pathway; the caspase-3 positive staining in the JAK1-overexpression, STAT3-overexpression, and the Ai Da Lotion intervention groups was significantly weakened, with a significant reduction in the number and intensity of positive cells, indicating that the Ai Da Lotion intervention group could effectively attenuated cell apoptosis. These findings collectively

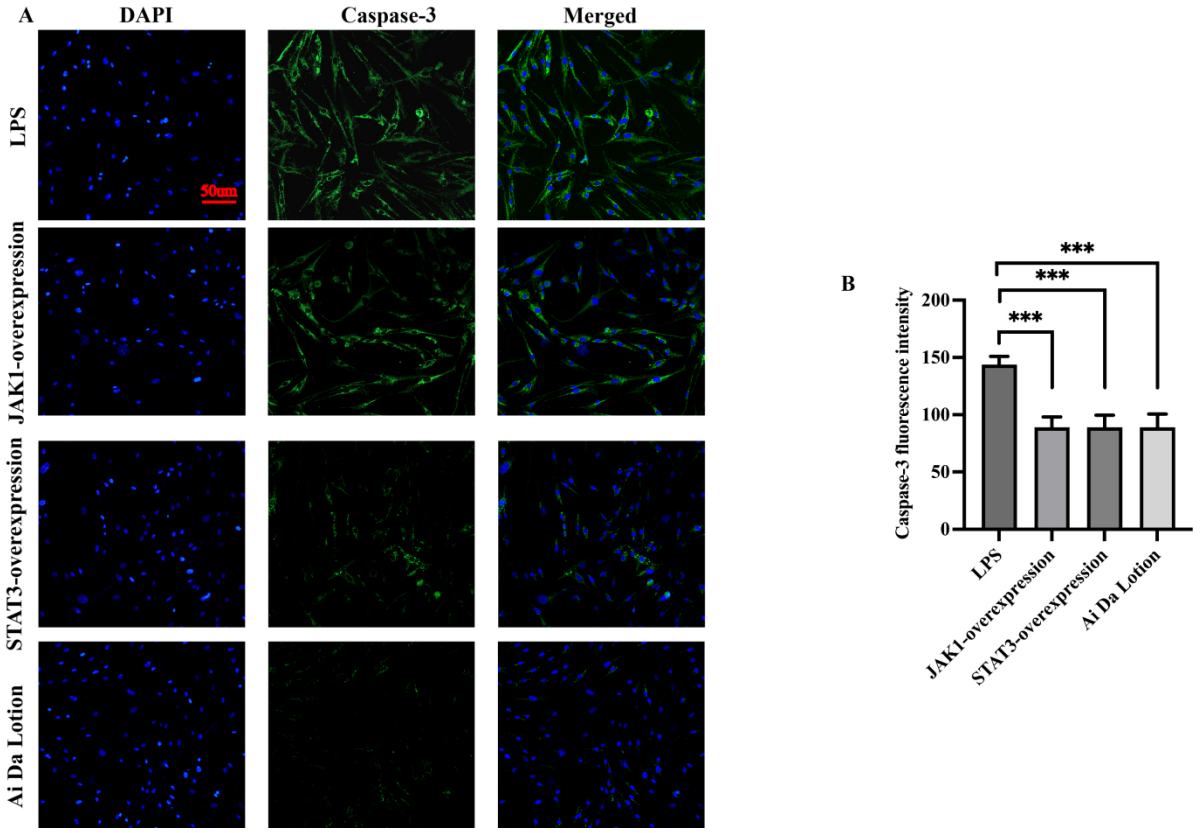

Figure 9. Immunofluorescence detection of caspase-3 (apoptosis marker) with representative images and statistical analysis. (A) Representative immunofluorescence images of DAPI (blue; nuclear staining) and cleaved caspase-3 (green; apoptosis marker) in the LPS group, JAK1-overexpression group, STAT3-overexpression group, and Ai Da Lotion group (scale bar = 50 μm; magnification = 20×). (B) Quantitative analysis of cleaved caspase-3 fluorescence intensity. Data are presented as mean ± standard deviation (n = 3 independent experiments). Statistical significance is indicated as ***$p <$ 0.001 vs. LPS group.

Abbreviations: DAPI: 4',6-diamidino-2-phenylindole; JAK1: Janus kinase 1; LPS: Lipopolysaccharide; STAT3: Signal transducer and activator of transcription 3.

indicate that Ai Da Lotion can regulate the JAK1/STAT3 signaling pathway and downregulate the expression of the apoptotic executor molecule caspase-3, thereby inhibiting LPS-induced keratinocyte apoptosis, reducing epidermal barrier damage and inflammatory responses, and exerting its therapeutic effect on eczema-like skin lesions.

4. Discussion

By combining chemical profiling, network pharmacology, and functional validation, this study defines a mechanistic framework for Ai Da Lotion in treating eczema. To our knowledge, these findings provide the first molecular evidence that this TCM formulation reduces skin inflammation and improves barrier dysfunction by modulating the JAK1/STAT3 signaling axis,[29,30] and offer a model for clarifying the therapeutic rationale of polyherbal medicines.

4.1. Chemical complexity and rational standardization

The identification of 889 constituents underscores the polypharmaceutical nature of Ai Da Lotion, yet chemical richness presents standardization challenges. Our Lipinski-compliant screening distilled 42 bioactive compounds, among which 8-deoxylactucin and 6β-hydroxymethandrostenolone emerged as high-affinity JAK1/STAT3 ligands despite structural divergence.[29] This structural diversity, rather than redundancy, likely underpins multi-target synergy—a hallmark of effective TCM formulas.[1,31] The enrichment strategy not only streamlined mechanistic investigation but also may provide quantitative quality markers for future batch-to-batch consistency.

4.2. Systems-level revelation of JAK1/STAT3 as a nodal hub

Network analysis revealed robust interconnectivity among

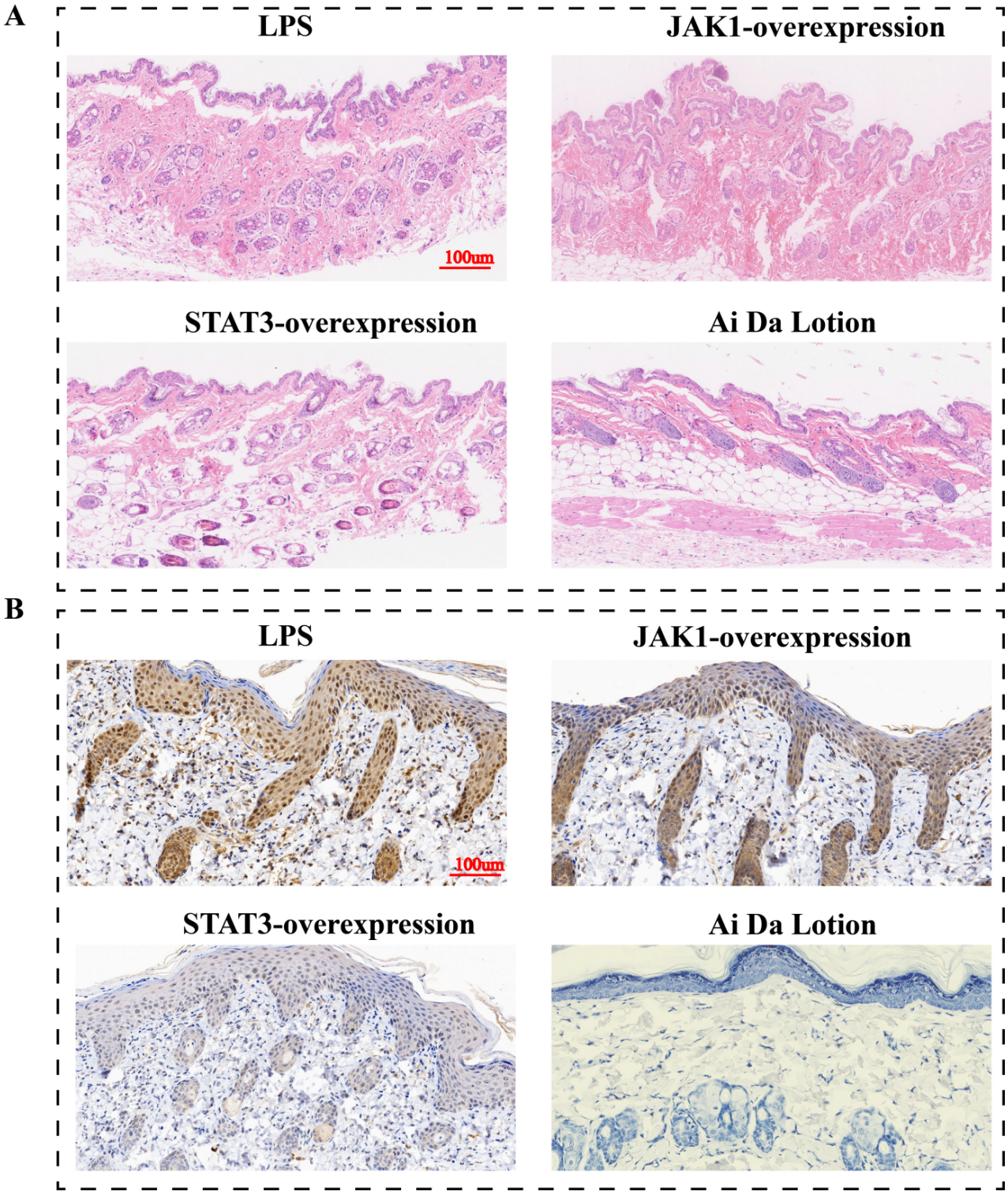

Figure 10. Representative images of (A) hematoxylin and eosin staining show the epidermal structure, degree of hyperkeratosis, and infiltration of inflammatory cells in the skin/ear tissues across groups, and (B) immunohistochemical staining show the expression and distribution of activated caspase-3 (brown-yellow positive signal) across groups (scale bar = 100 μm; magnification = 10×).
Abbreviations: JAK1: Janus kinase 1; LPS: Lipopolysaccharide; STAT3: Signal transducer and activator of transcription 3.

37 therapeutic targets ($p < 1 \times 10^{-16}$), with JAK1 and STAT3 forming a central regulatory module alongside tyrosine kinase 2 and STAT1.[32] While GO terms confirmed expected immunomodulatory functions, the enrichment of viral disease pathways (e.g., Measles, Chagas) highlights a deeper insight: these pathways converge on Th1/Th2 dysregulation and STAT3 hyperactivation, mirroring eczema's core immunopathology.[33,34] Notably, JAK1/STAT3 remained underrepresented in conventional KEGG inflammatory pathways annotations demonstrating network pharmacology's capacity to uncover latent therapeutic nodes that conventional enrichment overlooks.

4.3. Mechanistic validation and bidirectional regulation

Cellular assays and a mouse model of skin inflammatory injury corroborated network predictions: JAK1/STAT3 overexpression rescued LPS-impaired wound healing, while Ai Da Lotion recapitulated this effect via three coordinated mechanisms—enhancing EdU incorporation (proliferation), suppressing ROS/JC-1 depolarization (mitochondrial protection), and reducing caspase-3 activation (anti-apoptosis).[35] This functional triad aligns with STAT3's transcriptional repertoire (Bcl-xL, cyclin D1);[4] however, Ai Da Lotion's effect is not simple pathway activation. Rather, it suppresses pathological hyperphosphorylation while restoring physiological oscillatory activation—a nuanced "bidirectional tuning" that distinguishes TCM formulas from synthetic inhibitors and may explain its favorable safety profile.

4.4. Clinical translation and comparative advantages

Current eczema therapies face limitations: topical corticosteroids cause atrophy, while systemic JAK inhibitors carry thromboembolic risks.[6,7] Ai Da Lotion, as a topical preparation with low systemic absorption, demonstrates comparable efficacy (clinical data: 94.7% effectiveness, 58% reduced relapse) without systemic toxicity. The 42 active components, each with documented anti-inflammatory, antioxidant, or barrier-repair properties, achieve additive effects at sub-toxic concentration—a "low-dose multi-hit" strategy that modern drug development increasingly emulates.

4.5. Limitations and future directions

While this study provides robust multi-level evidence, our approach has constraints. Database-dependent target predictions necessitate orthogonal validation via surface plasmon resonance/isothermal titration calorimetry. Molecular docking lacks dynamic conformational context; future molecular dynamics simulations will assess complex stability. The LPS model captures acute inflammation but not chronic eczema features (e.g., Th2/Th22 polarization, fibrosis), requiring validation in Der p1 or MC903-induced models.[36,37] The precise molecular locus of Ai Da Lotion's JAK1/STAT3 modulation[24,38]—whether via SH2 domain competition, phosphatase recruitment, or epigenetic regulation—demands phosphoproteomic and site-directed mutagenesis studies. Additionally, the formulation's dermal pharmacokinetics and metabolic fate remain uncharacterized, which limits the ability to optimize clinical dosing strategies.

Future work should employ conditional knockout mice (K14-Cre;Stat3$^{fl/fl}$) to dissect skin-specific versus systemic STAT3 functions, conduct head-to-head trials against JAK inhibitors, and develop "formula–monomer" hybrid therapies that preserve synergistic benefits while enhancing pharmaceutical properties.

5. Conclusion

This study elucidated Ai Da Lotion's "multi-component—JAK1/STAT3 axis—multi-effect" therapeutic paradigm, establishing a translational roadmap for TCM modernization. Beyond identifying a druggable pathway, we revealed a holistic modulation strategy that restores immune homeostasis rather than inducing blunt immunosuppression—a conceptual framework relevant to complex chronic diseases beyond dermatology.

Acknowledgments

We gratefully acknowledge the assistance and instruction from Hainan Institute of Materia Medica and Hainan Medical University.

Funding

This research was supported by Hainan Provincial Natural Science Foundation of China (823MS155), Hainan Provincial Key R&D Project (ZDYF2025SXLH015), and Hainan Province Scientific Research Projects of Higher Education Institutions in 2023 (Hnky2023-31).

Conflict of interest

The authors declare they have no competing interests.

Author contributions

Conceptualization: Jing Lin
Formal analysis: Yuan Li
Investigation: Zixiao Jiang
Methodology: Yangyang Liu
Writing–original draft: Yuan Li
Writing–review & editing: Haolin Wu

Ethics approval and consent to participate

The animal study protocol was approved by the Experimental Animal Ethics Committee of Hainan Institute of Materia Medica Co., Ltd (ethical lot number: 2024HL0005). All experimental procedures were conducted in accordance with the relevant guidelines and regulations for the care and use of laboratory animals, including but not limited to the National Institutes of Health Guide for the Care and Use of Laboratory Animals. All efforts were made to minimize animal suffering and to reduce the number of animals used.

Consent for publication

Not applicable.

Availability of data

Data are available from the corresponding author upon reasonable request.

References

1. Kwon HE, Ahn HJ, Jeong SJ, *et al*. The increased prevalence of keloids in atopic dermatitis patients with allergic comorbidities: a nationwide retrospective cohort study. *Sci Rep*. 2021;11(1).

   doi: 10.1038/s41598-021-03164-4

2. Apfelbacher C, Bewley A, Molin S, *et al*. Prevalence of chronic hand eczema in adults: a cross-sectional survey of over 60 000 respondents from the general population of Canada, France, Germany, Italy, Spain and the UK. *Br J Dermatol*. 2025;192(6):1047-1054.

   doi: 10.1093/bjd/ljaf020

3. Maspero J, De Paula Motta Rubini N, Zhang J, *et al*. Epidemiology of adult patients with atopic dermatitis in AWARE 1: A second international survey. *World Allergy Organ J*. 2023;16(3):100724.

   doi: 10.1016/j.waojou.2022.100724

4. Agilan B, Rajendra Prasad N, Kanimozhi G, *et al*. Caffeic Acid Inhibits Chronic UVB-Induced Cellular Proliferation Through JAK-STAT3 Signaling in Mouse Skin. *Photochem Photobiol*. 2016;92(3):467-474.

   doi: 10.1111/php.12588

5. Fargnoli MC, Molin S, Bewley A, *et al*. Moderate to severe Chronic Hand Eczema in clinical practice: etiological subtypes, clinical signs and symptoms, and comorbidities—results from the RWEAL study. *J Dermatolog Treat*. 2026;37(1).

   doi: 10.1080/09546634.2025.2603121

6. Tsai SYC, Phipatanakul W, Hawryluk EB, *et al*. Comparative safety of oral Janus kinase inhibitors versus dupilumab in patients with atopic dermatitis: A population-based cohort study. *J Allergy Clin Immunol*. 2024;154(5):1195-1203.e3.

   doi: 10.1016/j.jaci.2024.07.019

7. Benandi K, Spires A, Hansen A, Linfante A. Systemic risk profiles of topical ruxolitinib and oral Janus kinase inhibitors in patients with atopic dermatitis: A retrospective cohort study from the TriNetX network. *J Am Acad Dermatol*. 2025;93(4):1035-1041.

   doi: 10.1016/j.jaad.2025.06.058

8. Singleton H, Hodder A, Almilaji O, *et al*. Educational and psychological interventions for managing atopic dermatitis (eczema). *Cochrane Database Syst Rev*. 2024;2024(8).

   doi: 10.1002/14651858.cd014932.pub2

9. Hallit S, Haddad C, Zeidan RK, *et al*. Cognitive function among schoolchildren in Lebanon: association with maternal alcohol drinking and smoking during pregnancy and domestic use of detergents and pesticides during childhood. *Environ Sci Pollut Res*. 2019;26(14):14373-14381.

   doi: 10.1007/s11356-019-04797-9

10. Drucker AM, Morra DE, Prieto-Merino D, *et al*. Systemic Immunomodulatory Treatments for Atopic Dermatitis. *JAMA Dermatol*. 2022;158(5):523.

    doi: 10.1001/jamadermatol.2022.0455

11. Yori F, Sarmiento C, Gimeno Beltran J, Umbert I. The Combination of Mineral Salts and Natural Antioxidants Agents Is Highly Effective in Atopic Dermatitis. *Clin Cosmet Investig Dermatol*. 2025;18:3695-3711.

    doi: 10.2147/ccid.s562171

12. Zalewski A, Krajewski PK, Szepietowski JC. Psychosocial Consequences of Hand Eczema—A Prospective Cross-Sectional Study. *J Clin Med*. 2023;12(17):5741.

    doi: 10.3390/jcm12175741

13. Buske-Kirschbaum A, Trikojat K, Tesch F, *et al*. Altered hypothalamus-pituitary-adrenal axis function: A relevant factor in the comorbidity of atopic eczema and attention deficit/hyperactivity disorder? *Psychoneuroendocrinology*. 2019;105:178-186.

    doi: 10.1016/j.psyneuen.2018.12.005

14. Matthewman J, Schultze A, Strongman H, *et al*. Cohort studies on 71 outcomes among people with atopic eczema in UK primary care data. *Nat Commun*. 2024;15(1).

    doi: 10.1038/s41467-024-54035-1

15. Rao H, Tan JBL. Polysaccharide-based hydrogels for atopic dermatitis management: A review. *Carbohydr Polym*. 2025;349:122966.

    doi: 10.1016/j.carbpol.2024.122966

16. Paz M, Lio P. Skin-Immune-Neuro-Gastro-Endocrine (SINGE) System: Lighting the Fire on Atopic Dermatitis

Research. *Dermatol Pract Concept*. 2025;15(4):5329.

doi: 10.5826/dpc.1504a5329

17. Wang X, Meng J, Wu Q, Feng J, Jing H. Clinical Efficacy of Integrated Traditional Chinese and Western Medicine in the Treatment of Eczema: A Meta-Analysis. *Comput Math Methods Med*. 2022;2022:1-7.

doi: 10.1155/2022/7202626

18. Gao W, Qiao X, Zhu J, *et al*. Clinical Efficacy of Tacrolimus Ointment + 3% Boric Acid Lotion Joint Chinese Angelica Decoction in Chronic Perianal Eczema. *Comput Math Methods Med*. 2021;2021:1-5.

doi: 10.1155/2021/1016108

19. Law SK, Wang Y, Wu XX. Comparison of the Effectiveness Differences between Western and Chinese Medicinal Ointments against Eczema. *Pharmaceuticals*. 2025;18(9):1248.

doi: 10.3390/ph18091248

20. Uzun S, Wang Z, McKnight TA, *et al*. Improvement of skin lesions in corticosteroid withdrawal-associated severe eczema by multicomponent traditional Chinese medicine therapy. *Allergy Asthma Clin Immunol*. 2021;17(1).

doi: 10.1186/s13223-021-00555-0

21. Ahuja A, Gupta J, Gupta R. Miracles of Herbal Phytomedicines in Treatment of Skin Disorders: Natural Healthcare Perspective. *Infect Disord Drug Targets*. 2023;23(3):328-338.

doi: 10.2174/1871526520666200622142710

22. Wan HL, Chen HZ, Shi XQ. Study on effect of Traditional Chinese Medicine Jianpi Chushi decoction and ointment on chronic eczema. *Asian Pac J Trop Med*. 2016;9(9):920-923.

doi: 10.1016/j.apjtm.2016.07.019

23. Blauvelt A, Silverberg JI, Lynde CW, *et al*. Abrocitinib induction, randomized withdrawal, and retreatment in patients with moderate-to-severe atopic dermatitis: Results from the JAK1 Atopic Dermatitis Efficacy and Safety (JADE) REGIMEN phase 3 trial. *J Am Acad Dermatol*. 2022;86(1):104-112.

doi: 10.1016/j.jaad.2021.05.075

24. Kasap N, Kara A, Celik V, *et al*. Atypical Localization of Eczema Discriminates DOCK8 or STAT3 Deficiencies from Atopic Dermatitis. *J Clin Immunol*. 2023;43(8):1882-1890.

doi: 10.1007/s10875-023-01554-z

25. Zhang T, Huang J, Zhang Z, *et al*. Flow cytometry and 5-ethynyl-2'-deoxyuridine (EdU) labeling to detect the cell cycle dynamics of Phaeodactylum tricornutum under light. *J Phycol*. 2022;58(4):555-567.

doi: 10.1111/jpy.13250

26. De Biasi S, Gibellini L, Cossarizza A. Uncompensated Polychromatic Analysis of Mitochondrial Membrane Potential Using JC-1 and Multilaser Excitation. *Curr Protoc Cytom*. 2015;72(1).

doi: 10.1002/0471142956.cy0732s72

27. Zhang S, Ye C, Guo L, *et al*. iLOV3.0 Fluorescent Probes for Monitoring ROS Changes in Mammalian Cells. *Bioconjug Chem*. 2025;36(8):1709-1720.

doi: 10.1021/acs.bioconjchem.5c00208

28. Wang F, Deng H, Zhou M, *et al*. Anti-PD-1 exacerbates bleomycin-induced lung injury in mice via Caspase-3/GSDME-mediated pyroptosis. *Cell Death Dis*. 2025;16(1).

doi: 10.1038/s41419-024-07319-9

29. Luo Z, Liu X, Xu C, *et al*. Exploring the mechanism of Zanthoxylum bungeanum essential oil in alleviating acute pruritus in rats based on network pharmacology, molecular docking, and experimental pharmacology. *J Ethnopharmacol*. 2026;357:120889.

doi: 10.1016/j.jep.2025.120889

30. Dadi H, Jones TA, Merico D, *et al*. Combined immunodeficiency and atopy caused by a dominant negative mutation in caspase activation and recruitment domain family member 11 (CARD11). *J Allergy Clin Immunol*. 2018;141(5):1818-1830.e2.

doi: 10.1016/j.jaci.2017.06.047

31. Chen M, Wang Y, Wang M, *et al*. Keratin 6A promotes skin inflammation through JAK1-STAT3 activation in keratinocytes. *J Biomed Sci*. 2025;32(1).

doi: 10.1186/s12929-025-01143-9

32. Dorjbal B, Stinson JR, Ma CA, *et al*. Hypomorphic caspase activation and recruitment domain 11 (CARD11) mutations associated with diverse immunologic phenotypes with or without atopic disease. *J Allergy Clin Immunol*. 2019;143(4):1482-1495.

doi: 10.1016/j.jaci.2018.08.013

33. Mokaram Doust Delkhah A. Identification of STAT3 signaling as a shared pathogenic signature in systemic lupus erythematosus, chronic obstructive pulmonary disease, and asthma. *Sci Rep*. 2025;15(1).

doi: 10.1038/s41598-025-07184-2

34. Niehues T, von Hardenberg S, Velleuer E. Rapid identification of primary atopic disorders (PAD) by a clinical landmark-guided, upfront use of genomic sequencing. *Allergol Select*. 2024;8(01):304-323.

doi: 10.5414/ALX02520E

35. Aramwit P, Fongsodsri K, Tuentam K, *et al*. Sericin coated thin polymeric films reduce keratinocyte proliferation via the mTOR pathway and epidermal inflammation through

IL17 signaling in psoriasis rat model. *Sci Rep*. 2023;13(1).

doi: 10.1038/s41598-023-39218-y

36. Brewer MG, Yoshida T, Kuo FI, *et al*. Antagonistic Effects of IL-4 on IL-17A-Mediated Enhancement of Epidermal Tight Junction Function. *Int J Mol Sci*. 2019;20(17):4070.

doi: 10.3390/ijms20174070

37. De La Cruz NC, Mockel M, Niehues H, *et al*. Ex Vivo Infection of Human Skin Models with Herpes Simplex Virus 1: Accessibility of the Receptor Nectin-1 during Formation or Impairment of Epidermal Barriers Is Restricted by Tight Junctions. *J Virol*. 2023;97(6).

doi: 10.1128/jvi.00262-23

38. Na K, Lkhagva-Yondon E, Kim M, *et al*. Oral treatment with Aloe polysaccharide ameliorates ovalbumin-induced atopic dermatitis by restoring tight junctions in skin. *Scand J Immunol*. 2019;91(3).

doi: 10.1111/sji.12856